Multiple four-wave mixing in optical fibers: 1.5–3.4-THz femtosecond pulse sources and real-time monitoring of a 20-GHz picosecond source

J. Fatome [a],[*], S. Pitois [a], C. Fortier [a], B. Kibler [a], C. Finot [a], G. Millot [a], C. Courde [b], M. Lintz [b], E. Samain [c]

[a] *Institut Carnot de Bourgogne, UMR 5209 CNRS-Université de Bourgogne, 9 av. Alain Savary, 21078 Dijon, France*
[b] *Université de Nice Sophia-Antipolis, CNRS, Observatoire de la Côte d'Azur, Laboratoire ARTEMIS, Boulevard de l'Observatoire, 06304 Nice Cedex 04, France*
[c] *GeoAzur, Université de Nice Sophia-Antipolis, CNRS, Observatoire de la Côte d'Azur, 2130 Route de l'Observatoire, 06460 Caussols, France*

ABSTRACT

In this work, we report recent progress on the design of all-fibered ultra-high repetition-rate pulse sources for telecommunication applications around 1550 nm. The sources are based on the non-linear compression of an initial beat-signal through a multiple four-wave mixing process taking place into an optical fiber. We experimentally demonstrate real-time monitoring of a 20 GHz pulse source having an integrated phase noise 0.01 radian by phase locking the initial beat note against a reference RF oscillator. Based on this technique, we also experimentally demonstrate a well-separated high-quality 110 fs pulse source having a repetition rate of 2 THz. Finally, we show that with only 1.4 m of standard single mode fiber, we can achieve a twofold increase of the repetition rate, up to 3.4 THz, through the self-imaging Talbot effect. Experimental results are supported by numerical simulations based on the generalized non-linear Schrödinger equation.

© 2010 Elsevier B.V. All rights reserved.

1. Introduction

Generation of high-quality high repetition rate optical pulse trains around 1550 nm has become of a great interest in many scientific applications such as optical sampling [1,2], ultra-high capacity transmission systems [3,4], optical switching [5], optical clock generation [6], component testing, metrology or non-linear phenomena studies [7–9]. Unfortunately, the current bandwidth limitations of optoelectronic devices prevent the direct generation of pulses with repetition rate higher than 50 GHz and with a temporal width below a few picoseconds. In order to overcome the limit of electronic bandwidth, mode-locked fiber lasers could be employed [10,11]. A second, attractive and all-optical non-linear method is based on the adiabatic transformation of a sinusoidal beat-signal into well-separated pulses through its non-linear compression in optical fibers. The pulse repetition rate of the source is then simply determined by the frequency of the initial beating. This all-optical approach has been successfully demonstrated with various experimental setups including dispersion-decreasing fibers [12], adiabatic Raman compression in standard optical fibers [13] and step-like or comb-like dispersion profiled fibers [14–19]. However, these techniques often require relatively complicated fiber

map arrangement via numerous reshaping stages based on a careful longitudinal dispersion management using custom designed optical fibers. More recently, this non-linear compression effect has been observed through a multiple four-wave mixing (MFWM) process taking place within an anomalous dispersive optical fiber [20,21]. This last method has been proved to be an attractive and efficient alternative way to generate very high repetition-rate pulse trains, combining both stability and simplicity of the experimental setup [22–25]. This powerful method has been successfully used for the generation of a 1.3-ps high-quality pulse train at 160 GHz and subpicosecond pulses up to 1 THz [25]. Combined with a second stage of compression based on the parabolic reshaping taking place into a normal dispersive optical fiber, we have also demonstrated that pulse sources with lower duty-cycle (up to 1/17) could be obtained at various repetition rates [26,27]. In this work, we report several recent and significant advances on the design of this kind of all-fibered ultra-high repetition-rate pulse sources for telecommunication applications in the C-band. In particular, for the first time of our knowledge, thanks to a phase lock set-up stabilizing the initial 20-GHz beat note, we experimentally demonstrate a direct real-time monitoring of the multiple four-wave mixing compression stage on a 50-GHz optical sampling oscilloscope. We have also demonstrated a record ultra-high repetition pulse source of 2 THz with pulses as short as 110 fs and finally, by means of 1.4 m of standard single mode fiber, we succeed in

* Corresponding author.
E-mail address: Julien.Fatome@u-bourgogne.fr (J. Fatome).

achieving a twofold increase of the repetition rate up to 3.4 THz through the self-imaging Talbot effect.

2. Experimental setup

The typical experimental setup is sketched in Fig. 1. The initial beat-signal is obtained by the superposition of two continuous wave 1.55-μm external cavity laser diodes (ECL) frequency separated by the repetition rate of the source under test. A phase modulator, driven by a RF frequency of 130 MHz, is used to suppress the stimulated Brillouin scattering (SBS) effect occurring in the compression fiber. The resulting beat-signal is then amplified to the required average power [25] thanks to an Erbium doped fiber amplifier (EDFA) before injecting into the compression fiber. Note that the whole beat-signal generation stage is polarization maintaining in order to maximize the four-wave mixing process in the compression fiber. At the fiber output, the generated pulse train is characterized both in intensity and phase by means of a Second Harmonic Generation Frequency-Resolved Optical Gating (SHG-FROG) set-up and an optical spectrum analyzer (OSA) [28,29].

3. 1.5–2-THz pulse sources

3.1. 1.5-THz results

The initial 1.5-THz beating was first generated though the temporal superposition of the two ECLs at 1549.6 nm and 1561.5 nm. The resulting beat-signal was then amplified with an average power of 3.3 W before injection into a short segment of 29 m of commercially available highly non-linear fiber (HNLF). At 1550 nm, the HNLF fiber has the following parameters measured by the modulation instability technique described in Ref. [30]. Chromatic dispersion was $D = 0.8$ ps/nm km. In order to avoid any asymmetry in the pulse intensity profile, a small dispersion slope fiber was chosen: $S = 0.008$ ps/nm^2 km. Finally the non-linear Kerr coefficient was measured to $\gamma = 9.5$ W^{-1} km^{-1} and fiber losses $\alpha = 0.7$ dB/km. Note that the end of the HNLF was directly connected to the FROG set-up in order to prevent any pulse distortion due to propagation in single mode fiber pigtail.

The experimental results of the 1.5-THz pulse source are illustrated in Fig. 2. Fig. 2a presents the FROG characterization; the inset shows the experimental FROG trace. The intensity profile highlights very well-separated pulses with a full width at half maximum (FWHM) of only 115 fs for a peak power of 15 W. The pulse shape is quasi Gaussian, without notable pedestal. Note that the phase is almost constant along the pulses, which confirms that they are nearly transform-limited. We have also checked that the autocorrelation function does not exhibit any difference between the central and the intercorrelation peaks, indicating that the timing and amplitude jitter as well as pulse width variations are quite moderate [31,32]. To compare the experimental results with
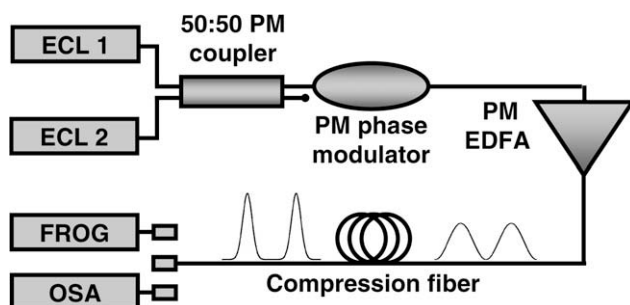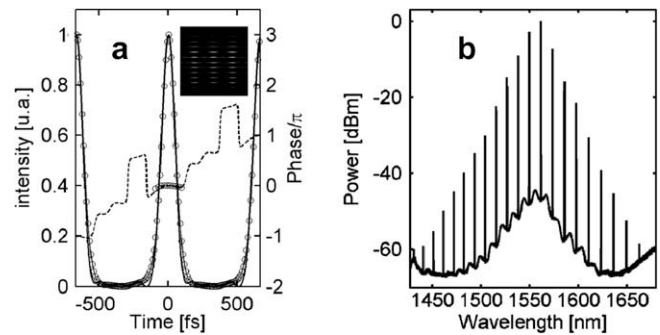
Fig. 2. FROG results for the 1.5-THz pulse train: (a) retrieved intensity profile (solid line), retrieved phase (dash line), simulation results (circles), inset shows the experimental FROG trace; (b) measured optical spectrum.

numerical predictions, we simulate the propagation in the fiber by means of the non-linear Schrödinger equation including the measured experimental fiber parameters and higher-order effects such as third-order dispersion, self-steepening and Raman scattering [33]. The results are plotted in circles: the experimental and numerical data are in excellent agreement, stressing an easy and reliable design of our source. We can notice a π phase shift between two consecutive pulses which originates from the initial beating and which is conserved during the whole compression stage in good agreement with numerical results. Our proposed source is therefore carrier suppressed. Fig. 1b shows the corresponding experimental spectrum of the 1.5-THz pulse train. We observe a broad frequency comb, resulting from the multiple four-wave mixing process taking place into the HNLF as well as spontaneous modulation instability provided by each frequency component of the spectrum, which is clearly visible in the spectral side lobes of each peak [7,23].

3.2. 1.7-THz and 2-THz results

Following general design rules [25], increasing the repetition rates imposes a shortening of the involved fiber and an increase of the average power. As a consequence, at 1.7 THz the optimum compression was achieved in only 16 m of HNLF fiber and for an input average power of 5.5 W. Fig. 3a illustrates the experimental results and presents the same features as those of Fig. 2. The retrieved intensity profile (solid line) shows well-separated pulses with a FWHM of about 110 fs in good agreement with numerical simulations (circles). Fig. 3b shows the result obtained for the 2-THz pulse source in the same segment of fiber and for an average power of 5.3 W. As in the previous result, the pulses (solid line) are clearly well-separated with a FWHM of 110 fs and are fully

Fig. 1. Experimental setup: PM: polarization maintaining.
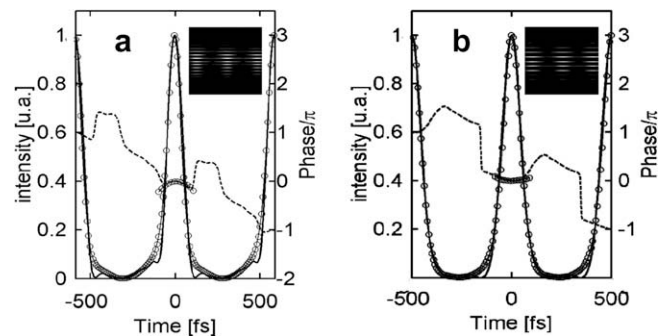
Fig. 3. (a) FROG results for the 1.7-THz pulse train: retrieved intensity profile (solid line), retrieved phase (dashed line), simulation results (circles), inset shows the experimental FROG trace; (b) same for the 2-THz pulse train.
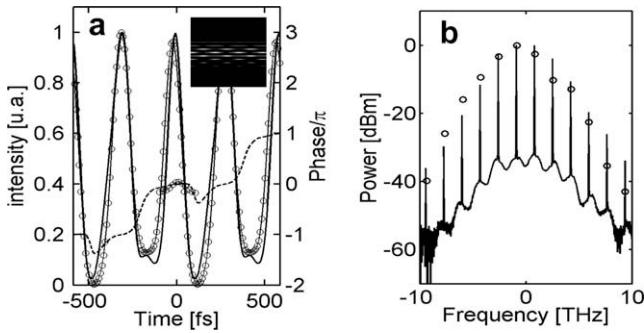
Fig. 4. FROG results for the Talbot based 3.4 THz pulse source: (a) retrieved intensity profile (solid line), retrieved phase (dashed line), simulation results (circles), inset shows the experimental FROG trace; (b) optical spectrum, experimentally recorded (solid line) and calculated from the retrieved intensity and phase (circles).

consistent with the numerical results (circles). Finally, the phase (dashed line) is quite flat along the pulses, indicating that they are nearly transform-limited.

4. Twofold multiplication of the repetition rate

In this section, we present the generation of a record 3.4-THz repetition-rate pulse source by means of a twofold multiplication of the bit rate through self-imaging Talbot effect [34]. In the temporal Talbot effect the spectral components of a pulse train that is incident upon a linearly dispersive element acquire phase delays that can cause either a regeneration of the original pulse train (integral self-imaging Talbot effect) or the generation of a pulse train at a multiple of the original repetition rate (fractional Talbot effect) [35–37].

In order to double the repetition rate of our 1.7-THz pulse source, we added in the experimental setup only 1.4 m of single mode fiber (SMF, D = 17 ps/nm/km, S = 0.055 ps/nm^2/km) following the HNLF compression fiber. The average power was reduced before injection into the SMF fiber in order to avoid any high-order soliton compression and ensure propagation in quasi pure dispersive regime. Fig. 4 shows the experimental results. Compared to Fig. 3a, the experimental results show a clear doubling of the rep-

etition rate. The pulses are clearly separated with a FWHM of 110 fs. A pretty good contrast is recorded, however an asymmetry could be noticed. This asymmetry is attributed to the third-order dispersion in the SMF segment as well as the initial asymmetry already present in the 1.7-THz pulse train, in good agreement with numerical predictions (circles).

5. Real-time monitoring of a 20 GHz pulse source

In parallels of ultra-high repetition-rate pulse sources, a phase-locked pulse source was developed at 20 GHz in order to perform a real-time observation of the pulse train emerging from the compressor and to monitor the non-linear dynamics as a function of the incident average power. To this aim, the initial beat-signal was phase-locked against a reference RF oscillator (see Fig. 5a). In addition to the frequency actuators of laser 2, an external phase modulator (ΦM1 in Fig. 5a) was used to improve the phase lock loop bandwidth to about 1 MHz. Fig. 5-b shows the transfer function of the phase lock loop. Not shown in the set-up, is the Smith predictor circuit [38] that compensates for the observed dead time in the operational amplifiers. The phase noise power spectrum density $S_\varphi^{SSB}(f)$ of the phase lock loop error signal can be integrated from 1 Hz to 1 MHz to give an integrated phase noise of 8×10^{-3} radian.

The resulting beat note was then amplified to 130 mW before injection into a length L = 7910 m of SMF (D = 17 ps/nm/km, S = 0.055 ps/nm^2/km, γ = 1.3 W^{-1} km^{-1}, losses α = 0.22 dB/km). Fig. 6 shows the signal of a 50-GHz photodiode monitoring the 20-GHz pulse train generated in the compressor. In order to eliminate any residual timing jitter, the 50-GHz sampling oscilloscope (see Fig. 5a) was triggered using a low-power (<1 mW) signal transmitted through a second fiber of identical length L. As the oscilloscope cannot be triggered at 20 GHz, a latch circuit is used to convert the 20 GHz signal to a frequency of 303 MHz. The pulse shapes, characterized in real-time with our technique, are in excellent quantitative agreement with numerical predictions (Fig. 6a, circles) which take into account the time response of the photodetection system. The pulses are well-separated without noticeable pedestal, and the FWHM is found to be 11 ps. Moreover, as can be seen in Fig. 6b, the eye-diagram of the compressed pulses is clearly open and does not exhibit any large timing jitter.
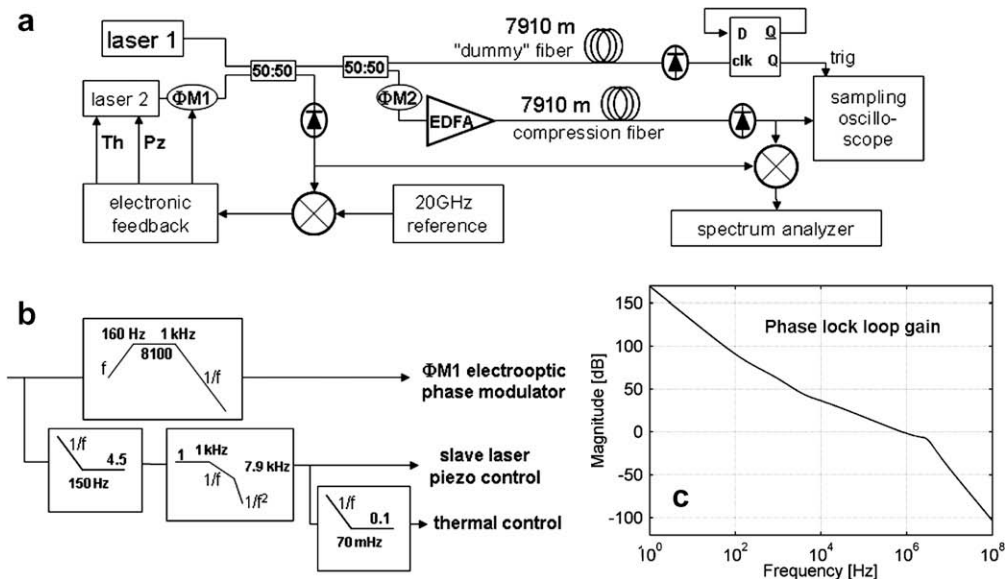
Fig. 5. (a) Set-up for real-time monitoring of the 20-GHz fiber compressor output, (b) transfer function of the feedback electronics and (c) total gain of the phase lock loop.
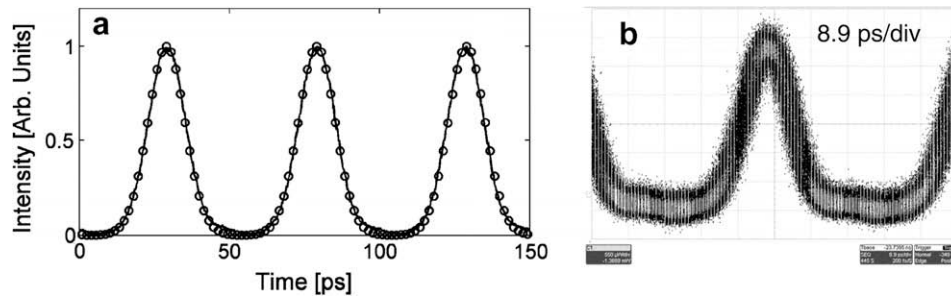
Fig. 6. (a) Intensity profile measured with a 50 GHz optical sampling oscilloscope (solid line) compared with numerical simulations (circles) for an input average power of 130 mW. (b) Eye-diagram of the 20 GHz-pulse train.
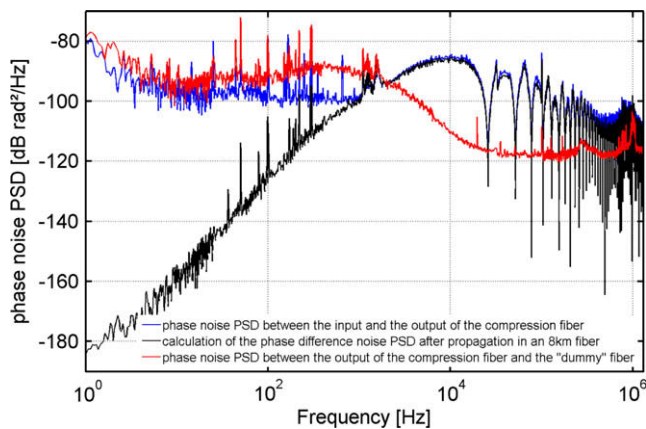
Fig. 7. Characterization of the phase noise power spectrum density of the output 20 GHz pulse source. Blue: noise recorded on the phase difference between the input of the EDFA and the output of the compressor. Black: calculated spectrum using Eq. (1) and the residual phase noise of the phase lock loop. Red: noise on the phase difference recorded between the output of the compressor and the output of the dummy 7910-m long fiber. (For interpretation of the references to colour in this figure legend, the reader is referred to the web version of this article.)

The phase of the pulses obtained at the output of the fiber compressor, with respect to the initial beat note, was characterized using a HF mixer and the spectrum analyzer shown in Fig. 5-a, in order to check for a possible noise added by the non-linear compression [39,40]. Using the measured power spectrum density (PSD) S_φ^{SSB} of the incoming beat note single sideband phase noise one can calculate the noise expected on the phase difference:

$$S_{\Delta\varphi(in/out)} = 4\sin^2(\pi f L/c)S_\varphi^{SSB} \qquad (1)$$

(green curve in Fig. 7). It qualitatively agrees with the measured PSD (blue curve in Fig. 7). In particular it shows marked zeroes at the frequencies which are integer multiples of the inverse of the propagation time in the fiber spool. The agreement fails at frequen-

cies lower than 1 kHz due to environmental contributions to the optical length: drifts of the ambient temperature give the dominant contribution to the phase noise at frequencies lower than 10 Hz, while between 10 Hz and 1 kHz acoustic perturbations dominate. Indeed the phase comparison of the signals obtained at the output of the two fiber spools (red curve in Fig 7) shows that, if some noise is added by the non-linear effects in the compression fiber or the EDFA, it does not exceed 2×10^{-6} radian/Hz$^{1/2}$ above 10 kHz.
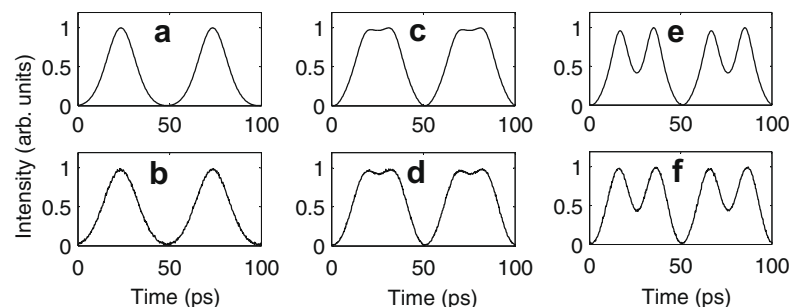
Finally, we have represented in Fig. 8b, d and f the experimental intensity profiles of the pulses emerging from the compression fiber for different input powers. These curves, recorded by means of the 50-GHz sampling oscilloscope, are compared with the intensity profiles obtained from numerical simulations and shown in Fig. 8a, c and e. At low-power (Fig. 8b), the initial beat-signal only undergoes a weak compression and the intensity profile of the pulses is nearly Gaussian. At stronger power than optimal, the peak of the pulses becomes nearly flat (Fig. 8d) and finally, at very high power, a dip occurs in the peak, leading to the generation of multipeak pulses, as can be seen in Fig. 8e [20]. These results are in very good agreement with numerical simulations.

6. Conclusion

In this work, we have reported recent progress on the design of all-fibered ultra-high repetition-rate pulse sources around 1550 nm. Based on the non-linear compression of an initial beating in optical fibers through a multiple four-wave mixing process, we have experimentally demonstrated that versatile high-quality pulse sources having repetition rates ranging from 20 GHz to 3.4 THz could be achieved. Thanks to an efficient control of the repetition rate though the phase lock of the initial beating against an RF reference we succeed, for the first time of our knowledge, to monitor the non-linear dynamics of the multiple four-wave mixing process occurring into the compression fiber. Finally, by means of the well-known self-imaging Talbot effect, we achieved to generate

Fig. 8. Intensity profile measured with a 50 GHz optical sampling oscilloscope (bottom) compared with numerical simulations (top). (a) and (b): 40 mW, (c) and (d): 250 mW, (e) and (f): 300 mW.

a 3.4-THz record repetition-rate pulse train with 110 fs full width at half maximum.

Acknowledgements

References

[1] P.A. Andrekson, M. Westlund, Laser Photon. Rev. 1 (2007) 231.
[2] H. Takara, S. Kawanishi, M. Saruwatari, Electron. Lett. 32 (1996) 1399.
[3] M. Nakazawa, T. Yamamoto, K.R. Tamura, Electron. Lett. 36 (2000) 2027.
[4] H.G. Weber, S. Ferber, M. Kroh, C. Schmidt-Langhorst, R. Ludwig, V. Marembert, C. Boerner, F. Futami, S. Watanabe, C. Schubert, Single channel 1.28 Tbit/s and 2.56 Tbit/s DQPSK transmission, ECOC 2005, Glasgow, Scotland, UK (Post-Deadline Paper Th 4.1.2).
[5] T. Yamamoto, E. Yoshida, M. Nakazawa, Electron. Lett. 34 (1998) 1013.
[6] G. Meloni, G. Berrettini, M. Scaffardi, A. Bogoni, L. Poti, M. Guglielmucci, Electron. Lett. 41 (2005) 1294.
[7] F.C. Cruz, Opt. Express 16 (2008) 3267.
[8] A. Bogoni, M. Scaffardi, P. Ghelfi, L. Poti, IEEE J. Sel. Top. Quantum Electron. 10 (2004) 1115.
[9] J. Fatome, S. Pitois, A. Kamagate, G. Millot, D. Massoubre, J.-L. Oudar, IEEE Photon. Technol. Lett. 19 (2007) 245.
[10] J. Schröder, S. Coen, F. Vanholsbeeck, T. Sylvestre, Opt. Lett. 31 (2006) 3489.
[11] J. Schröder, T.D. Vo, B.J. Eggleton, Opt. Lett. 34 (2009) 3902.
[12] P.V. Mamyshev, S.V. Chernikov, E.M. Dianov, IEEE J. Quantum Electron. 27 (1991) 2347.
[13] A. D'errico, C. Loiacono, M. Presi, G. Contestabile, E. Ciaramella, Widely tunable 40 GHz pulse source for 160 Gbit/s OTDM by simultaneous soliton generation and compression, ECOC'03, Rimini, Italy, Paper We 2.6.5, 2003.
[14] S.V. Chernikov, J.R. Taylor, R. Kashyap, Opt. Lett. 19 (1994) 539.
[15] S.V. Chernikov, J.R. Taylor, R. Kashyap, Electron. Lett. 30 (1994) 433.
[16] K. Igarashi, H. Tobioka, M. Takahashi, T. Yagi, S. Namiki, Electron. Lett. 41 (2005) 797.
[17] Y. Ozeki, S. Takasaka, T. Inoue, K. Igarashi, J. Hiroishi, R. Sugizaki, M. Sakano, S. Namiki, IEEE Photon. Technol. Lett. 17 (2005) 1698.
[18] Y. Ozeki, S. Takasaka, L. Hiroishi, R. Sugizaki, T. Yagi, M. Sakano, S. Namiki, Electron. Lett. 41 (2005) 1048.
[19] T. Inoue, S. Namiki, Laser Photon. Rev. 2 (2008) 83.
[20] S. Trillo, S. Wabnitz, T.A.B. Kennedy, Phys. Rev. A. 50 (1994) 1732.
[21] S. Pitois, J. Fatome, G. Millot, Opt. Lett. 27 (2002) 1729.
[22] J.F.L. Freitas, C.J.S. de Matos, A.S.L. Gomes, Simultaneous pulse train generation and wavelength conversion in a highly nonlinear fibre due to multiwave mixing, Presented at the ECOC 2005, Glasgow, UK, Paper Mo 4.5.5.
[23] A. Cerqueira Sodre, J.M. Chavez Boggio, A.A. Rieznik, H.E. Hernandez-Figueroa, H.L. Fragnito, J.C. Knight, Express 16 (2008) 2816.
[24] J. Fatome, S. Pitois, G. Millot, Electron. Lett. 41 (2005) 1391.
[25] J. Fatome, S. Pitois, G. Millot, IEEE J. Quantum Electron. 42 (2006) 1038.
[26] C. Finot, J. Fatome, S. Pitois, G. Millot, IEEE Photon. Technol. Lett. 19 (2007) 1711.
[27] C. Fortier, B. Kibler, J. Fatome, C. Finot, S. Pitois, G. Millot, Laser Phys. Lett. 5 (2008) 817.
[28] R. Trebino, K.W. Delong, D.N. Fittinghoff, J.N. Sweetser, M.A. Krumbugel, B.A. Richman, D.J. Kane, Rev. Sci. Instrum. 68 (1997) 3277.
[29] J. Fatome, S. Pitois, G. Millot, Opt. Fiber Technol. 10 (2004) 73.
[30] J. Fatome, S. Pitois, G. Millot, Opt. Fiber Technol. 12 (2006) 243.
[31] J. Fatome, J. Garnier, S. Pitois, M. Petit, G. Millot, M. Gay, B. Clouet, L. Bramerie, J.-C. Simon, Opt. Fiber Technol. 14 (2008) 84.
[32] M. Dinu, D.C. Kilper, H.R. Stuart, J. Lightwave Technol. 24 (2006) 1194.
[33] G.P. Agrawal, Nonlinear Fiber Optics, third ed., Academic Press, New York, 2001.
[34] J. Azaña, M.A. Muriel, IEEE J. Sel. Top. Quantum Electron. 7 (2001) 728.
[35] P. Petropoulos, M. Ibsen, M.N. Zervas, D.J. Richardson, Opt. Lett. 25 (2000) 521.
[36] J. Fatome, S. Pitois, G. Millot, Opt. Commun. 234 (2004) 29.
[37] J.A. Bolger, P. Hu, J.T. Mok, J.L. Blows, B.J. Eggleton, Opt. Commun. 249 (2005) 431.
[38] K. Warwick, D. Rees, Industrial Digital Control Systems, IET, second ed., 1988 (See section 4-6-6).
[39] M.D. Pelusi, T.D. Vo, F. Luan, S.J. Madden, D.-Y. Choi, D.A.P. Bulla, B. Luther-Davies, B.J. Eggleton, Opt. Express 17 (2009) 9314.
[40] M. Pelusi, F. Luan, T.D. Vo, M.R.E. Lamont, S.J. Madden, D.A. Bulla, D.-Y. Choi, B. Luther-Davies, B.J. Eggleton, Nat. Photon. 3 (2009) 139.